

## Microstructure Study of Aluminium Matrix Hybrid Composite Materials

Osman KEKLİK<sup>1\*</sup>, Hakan ADA<sup>2\*</sup>, Eren GÖNENÇ<sup>2\*</sup>, Nihat KAYA<sup>3\*</sup>

<sup>1</sup>Gazi University, Graduate School of Natural and Applied Sciences, Dept. of Met. and Materials Eng., Ankara, Türkiye.

<sup>2</sup>Gazi University, Faculty of Technology, Department of Met. and Materials Eng., Ankara, Türkiye.

<sup>3</sup>Osmaniye Korkut Ata University, Kadırlı Vocational School, Dept. of Machine Program, Osmaniye, Türkiye.

This study aims to produce aluminium matrix hybrid composite materials using Powder Metallurgy (PM) techniques and to investigate the microstructural properties of the resulting materials in detail. In the initial phase, various powder mixtures were processed using powder metallurgy and cold pressing methods, followed by sintering to complete the production of the composite materials. After their production, comprehensive examinations were conducted to analyze the microstructural characteristics of the composites. These investigations focused on the aluminium matrix reinforcement phases' distribution, size, morphology, and interfacial properties between the matrix and reinforcements. During this analysis, modern techniques such as Optical Microscopy (OM), Scanning Electron Microscopy (SEM), and X-ray Diffraction (XRD) were employed to perform in-depth microscopic and structural assessments of the samples.

**Keywords:** Aluminium, Powder metallurgy, Hybrid composite, Microstructure, SEM, XRD

Submission Date: 04 November 2024

Acceptance Date: 28 December 2024

\*Corresponding author: [hakanada@gazi.edu.tr](mailto:hakanada@gazi.edu.tr)

### 1. Introduction

Today, rapidly developing technologies in critical sectors such as defence, space, aviation, and automotive have led to the inadequacy of traditional materials and have made developing these materials mandatory. The material requirements arising from these technological advances constitute the main reason for producing composite materials with new and superior properties. The material requirements arising from these technological advances constitute the main reason for producing composite materials with new and superior properties [1,2].

The powder metallurgy method can be summarized as the process as the process of bonding very small particles together to form a single part.

This method is widely used in many fields, such as tungsten lamp wires, armour-piercing bullets, dental fillings and automotive powertrain gears. Powder metallurgy is an important method for producing metal matrix composites, metal alloys, and complex-shaped parts. This production method is frequently preferred in composite materials due to its advantages, such as offering superior microstructural properties and providing a certain degree of porosity and permeability [3]. Composite materials are a new type of material resulting from the combination of two or more materials that are insoluble with each other and have different properties. These materials can be combined into a single material by providing many properties that the constituent elements cannot have alone.

Composite materials consist of two main parts, the matrix and the reinforcing elements, and they can maintain their unique properties because they have interfaces within themselves [4]. Today, composite materials are widely used in many fields. The most common applications of these materials include sports equipment, electrical and electronic products, medical devices, and structural components in aircraft and ships [5,6]. Composite materials are divided into different categories according to the structure of the reinforcing elements: layered, mixed, fibre-reinforced and particle-reinforced.

In addition, according to the type of base material, they are classified as polymer, metal and ceramic-based composites [7,8]. Metal matrix composites combine metals with high ductility and toughness properties and high-strength ceramic materials. Metal matrix composite (MMC) materials are special composite structures that use a metal (such as Al, Ti, Mg, Fe, Cu) as the main matrix element and ceramics (such as  $B_4C$ , SiC,  $Al_2O_3$ , BN,  $Si_3N_4$ ) or carbon-based materials (such as fullerene, carbon nanotubes, graphene) as reinforcing elements [5,9]. AA2024, known for its lightweight and ductile properties and widely used in aerospace and defence industry studies, was preferred as the matrix material in this study. In AA2024 matrix composites, TiC,  $B_4C$ ,  $ZrO_2$ ,  $Al_2O_3$  and SiC are generally preferred as reinforcing elements [1,10]. Zirconia ( $ZrO_2$ ), one of these reinforcements, is a high-performance ceramic material with an important place in composite materials. Carbon nanotubes (CNT), which have recently been reinforced into composite materials as nanoparticles, are also important reinforcement materials that improve the properties of composite materials. Therefore, this study produced nanocomposites by reinforcing the matrix material with  $ZrO_2$  and CNTs, and the composite materials' microstructural properties were investigated.

Among metal matrix composite materials, the most preferred matrix material today is aluminium and its alloys. Aluminium is an ideal matrix material for MMCs in industrial applications due to its easy forming capacity, low density, good electrical and thermal conductivity, and high mechanical strength [1,5,9]. Al alloys have a wide range of applications in aerospace, automotive and structural applications [11,12]. AA2024 alloy stands out as one of the most widely used Al alloys for load-bearing components in aerospace, transportation and other industries due to its good machinability, high specific strength and heat resistance, high strength-to-weight ratio, high damage resistance and affordable price [13-15]. AA2024 is a high-strength Al-Cu-Mg alloy that can be strengthened by heat treatment. However, AA2024 alloys have disadvantages such as low strength, poor formability and corrosion resistance [16]. To overcome these problems, many researchers have carried out various studies [17-19]. In this context, ceramic-reinforced metal matrix composites have been developed to improve the performance of AA2024 [20-23]. However, despite these improvements, problems such as wettability of the matrix and ceramic reinforcement, porosity issues, and poor interface bonding have decreased mechanical properties [24,25]. Due to the

potential to overcome these challenges, there is a growing interest in metal/metal composites.

Carbon nanotubes (CNTs) are one of the advanced reinforcing elements that significantly impact composite materials. CNT is important in composite materials because it offers many advantages, such as high performance, lightweight, durability, and versatility. These properties make CNT a valuable material in modern engineering and design applications. CNT has exceptional mechanical properties. Despite their low density, they offer superior tensile and compressive strength, increasing the overall strength of composite materials and giving the material excellent thermal and electrical conductivity benefits. Despite their high strength, they have a low weight, enabling the production of lightweight composites, which is particularly advantageous in aerospace and automotive applications. Its resistance to the effects of many chemicals makes CNT an ideal choice as a reinforcement material for corrosion-resistant composites. CNT provides reinforcement by interacting with other materials in the composite matrix and strengthening the structure of the matrix. Thanks to their high solubility, they form compatible interfaces with the matrix. Thus, the microstructural properties of composite materials can be improved, leading to increased mechanical properties at the macro level [27,28].

$ZrO_2$ , like CNT, is a high-performance ceramic reinforcement material with an important place in composite materials.  $ZrO_2$  has a wide range of applications due to its mechanical strength, heat, and chemical resistance. It is a valuable material used in engineering applications.  $ZrO_2$  is known for its low density, high hardness and strength, ability to withstand high temperatures, low wear-high friction resistance, and good corrosion properties. This property increases the mechanical strength of composite materials, producing more durable, long-lasting, heat, wear and corrosion-resistant products. When  $ZrO_2$  is uniformly distributed within the composite matrix, it can generally contribute to improving physical properties at the macro level. This is particularly important in enhancing mechanical and electrical properties and allows  $ZrO_2$  to be used in combination with other materials in many applications to improve the properties of composites or give them special properties [29,30]. By reinforcing the AA2024 matrix with CNT and  $ZrO_2$ , whose superior properties are clearly stated above, significant improvements can be achieved towards producing advanced composite materials in many fields. Composites produced with combinations of CNT and  $ZrO_2$  can be particularly effective in enhancing mechanical, thermal and electrical properties and allow the development of high-performance materials for various industrial applications. The aim of this study is to develop lightweight materials with improved tensile, abrasion and fracture strength, high-temperature resistance, and high hardness with the production of AA2024/CNT/ $ZrO_2$  composite materials. Some noteworthy literature studies on CNT and  $ZrO_2$  composite materials with AA2024 matrix produced by powder metallurgy method are reported below. A study by T. Varol et al. [31] reported that  $B_4C$  nanocomposites with AA2024 matrix were successfully produced by the powder

metallurgy method.

In a study by Uyar et al. [32], composite structures were obtained by doping graphene and multi-walled CNTs into pure Cu, ZA27 and Al2024 matrices by powder metallurgy method. A study by Stergioudi [33] showed that the nanocomposites produced exhibited better performance in terms of compressive strength, elongation at break and microhardness compared to pure AA2024. A study by Channar et al. [34] revealed that Al<sub>2</sub>O<sub>3</sub>/SiC reinforcements in Al 2024-T6 alloy significantly improved the mechanical properties. Gök et al. [35] focused on improving the mechanical strength and wear resistance of aluminium matrix composites produced by powder metallurgy. A study by Sarmah and Gupta [36] investigated the mechanical properties of AA2024 aluminium/MWCNT nanocomposites produced using different powder metallurgy methods. Özerkan et al. [37] investigated the machinability of MWCNT-reinforced ZA27-based composites produced by powder metallurgy. Wei et al. [15] hybrid-modified AA2024 alloy with graphene nanoplates (GNPs) and ZrO<sub>2</sub> nanoparticles. Elbasuneey et al. [38] reported the continuous hydrothermal synthesis of colloidal ZrO<sub>2</sub> nanoparticles in artificial seawater as a corrosion inhibitor for AA2024. Singh et al. [39] focused on the properties of the hybrid composite of AA2024 with Al<sub>2</sub>O<sub>3</sub>/ZrO<sub>2</sub>/Gr.

The above literature studies have shown mechanical improvements in the AA2024 matrix and CNT and ZrO<sub>2</sub> reinforcements, which show the potential of improving the materials produced by powder metallurgy, while the literature studies on composite materials in which AA2024 matrix is reinforced with CNT and ZrO<sub>2</sub> are limited. In order to present an original study, the AA2024 matrix, CNT and ZrO<sub>2</sub> co-reinforced powder blends were produced by the PM method, and the microstructural characterization of the samples was determined. At the microstructural characterization stage, Optical Microscope (OM), Scanning Electron Microscope (SEM), and X-ray diffraction (XRD) examinations were performed on the samples prepared by metallography standards.

## 2. Experimental Studies

### 2.1. Materials

In this study, AA2024 alloy (0-100 mesh) was chosen as the matrix material due to its good processability, high specific strength and heat resistance, high strength-to-weight ratio, high wear and damage resistance, and CNT (28-48 nm) and ZrO<sub>2</sub> (20-30 nm) were chosen as reinforcement materials due to their important properties such as high performance, lightweight, durability and versatility. First, the powder mixtures were determined in the mixture ratios in Table 1, weighed on a precision balance and made ready for mixing.

**Table 1:** Mixing ratios of the powders used in the study

Specimen no	Material name	AA2024 (%)	ZrO <sub>2</sub> (%)	CNT (%)
1	Unreinforced AA2024	100	-	-
2	%94 AA2024 %6 ZrO <sub>2</sub>	94	6	-
3	%99,5 AA2024 %0.5 CNT	99,5	-	0,5
4	% 93,5 AA2024 %6 ZrO <sub>2</sub> %0.5 CNT	93,5	6	0,5

### 2.2. Method

The high-purity powders with the weight percentages given in Table 1 were subjected to the mechanical alloying process by mixing at 350 rpm mixing speed, 90 minutes mixing time and 1/10 powder/balls ratio in the Retsch brand PM100 model device. The mechanically alloyed powders were then cold pressed in a one-way axial press under 500 MPa pressure. After cold pressing, the samples were subjected to sintering in an atmosphere-controlled device at 550 °C for 2 hours and composite material production was completed.

The sample preparation phase started for OM, SEM, EDS and XRD examinations. The samples were bakelitized with ATM Opal 460 bakelite device at Gazi University Faculty of Technology, Department of Metallurgical and Materials Engineering and prepared for metallographic examinations by standard metallographic methods (sanding + polishing). Sanding operations were performed with ATM Saphir 330 devices using 240, 400, 800, and 1000 grit abrasives. Keller reagent, which is the etchant of aluminium and its alloys, was used as an etchant to expose the microstructures. After each etching process, the surface of the samples was sprayed with pure water and then dried by spraying alcohol. After etching, the samples were polished. 6 µm and 3 µm monocrystalline diamond suspension solutions and felts were used for polishing, respectively. The devices used in metallography processes are given in Figure 1. OM images of the metallographically prepared samples were imaged with a Leica DMI5000M device with a Leica DFC 320 digital camera, and SEM examinations were imaged with a Jeol brand and JSM-6060 LW model device. OM images were taken at magnification ratios of 200 and 500, and SEM images were taken at magnification ratios of 1000 and 2000. After the OM and SEM examinations, XRD examinations were performed on the samples. XRD analyses were performed on Bruker D8 Advance brand device at 10°- 90° 2θ angles.



**Figure 1:** Instruments used in metallography processes

### 3. Results and Discussion

The results and findings obtained within the scope of OM and SEM images and XRD analyses obtained from CNT and ZrO<sub>2</sub> reinforced composite materials together with unreinforced AA2024 alloy produced within the scope of this study are given in the following titles, respectively.

#### 3.1. Microstructure Investigations

OM images obtained from composite materials with AA2024 matrix and CNT - ZrO<sub>2</sub> reinforced composites are given in Figure 2. In the OM images, S1 shows a homogeneously distributed matrix structure containing 100% AA2024 alloy. The fact that there are visibly few pores and/or secondary phases in the structure indicates that the sintering process and the interface form are as expected. Again, in the unreinforced AA2024 alloy, the grains are clearly distinguishable, and the phase boundaries are well-defined. In the OM images of 6% ZrO<sub>2</sub> reinforced S2 alloy, it is observed that ZrO<sub>2</sub> particles are dispersed in the AA2024 matrix and form dark areas. Considering that the reinforcement particle is nano-sized, it can be said that the imaged structures contain agglomerated ZrO<sub>2</sub> particles. These particles were not homogeneous in the matrix but clustered in places. This may indicate problems such as incomplete dispersion of the reinforcement material or agglomeration (clumping). Sample S3 is a composite material made of 99.5% AA2024 alloy with 0.5% CNT reinforcement. As known from the literature, CNT usually forms fine and reticulated structures. It can be interpreted that some dark regions in the OM image indicate the clustering of CNT or accumulation in intergranular areas. Although CNT is added in low percentages, it is a reinforcing element that makes it difficult to achieve homogeneous distribution. Therefore, in the production of composite materials, ensuring the homogeneous distribution of CNT in the matrix is very important for the properties of composite materials.

In the OM image, it was determined that CNT was not completely dispersed and formed some local densities in places. Sample S4 shows the microstructure of 93.5% AA2024, 6% ZrO<sub>2</sub> and 0.5% CNT-reinforced hybrid composite material. The microstructure image shows that ZrO<sub>2</sub> and CNT reinforcements are distributed in black areas within the matrix structure. Agglomeration of ZrO<sub>2</sub> and localized densification of CNT are observed in the images. It is also thought that using two different reinforcements together may make homogeneous distribution more difficult. Especially the particle density and clusters formed in the hybrid structure can be attributed to a bonding

weakness that may arise from the matrix-reinforcement interface or micro cracks formed during processing.

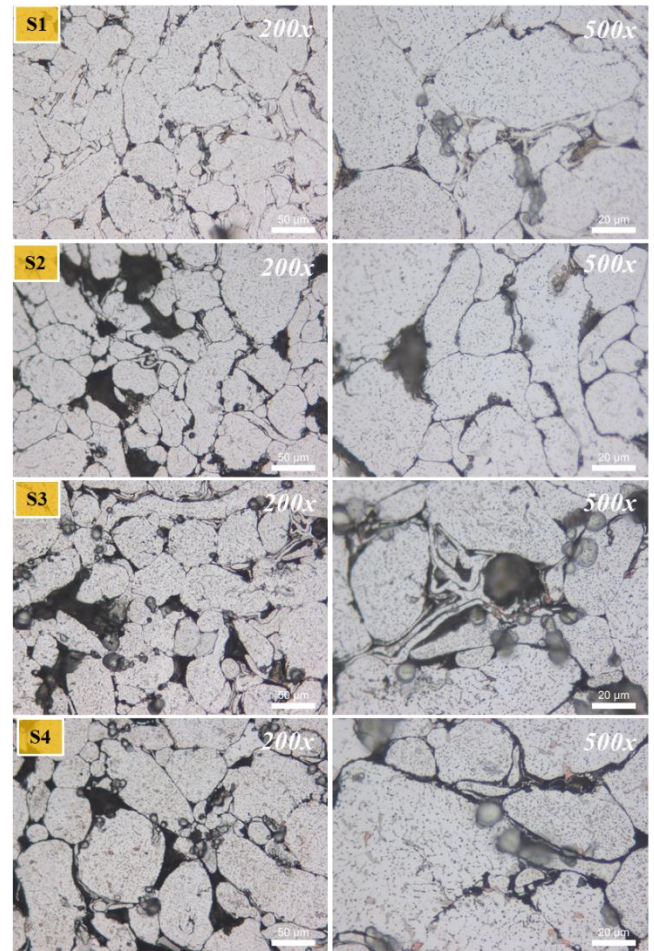


**Figure 2:** OM images of composite materials (S1: %100 AA2024, S2: %94 AA2024, %6 ZrO<sub>2</sub>, S3: %99,5 AA2024, %0,5 CNT, S4: %93,5 AA2024, %6 ZrO<sub>2</sub>, %0,5 CNT).

SEM images obtained from composite materials with AA2024 matrix and CNT - ZrO<sub>2</sub> reinforced composites are given in Figure 3. In the SEM images, samples with four different chemical compositions are shown at high magnifications of 1000x and 2000x. Sample S1, which contains 100% AA2024 alloy, exhibited a homogeneous structure as in SEM images. The grain boundaries are clearly visible in the images, and no second phase or reinforcement particles were observed. The small amount of micro cracks or pore marks in the SEM images are generally natural micro defects that may occur during material production and are not abnormal in size. In the SEM images of sample S2, many shiny, rod-like or diffusely dispersed white phases were observed. These reflect the typical visual characteristics of ZrO<sub>2</sub> particles in SEM. Although ZrO<sub>2</sub> appears to be homogeneously dispersed in the matrix, agglomeration of particles was also noticed. The accumulation of these particles at the grain boundaries and within the matrix can locally affect the material properties, making pores or micro cracks more pronounced. The presence of reinforcement can also cause bonding difficulties during machining.

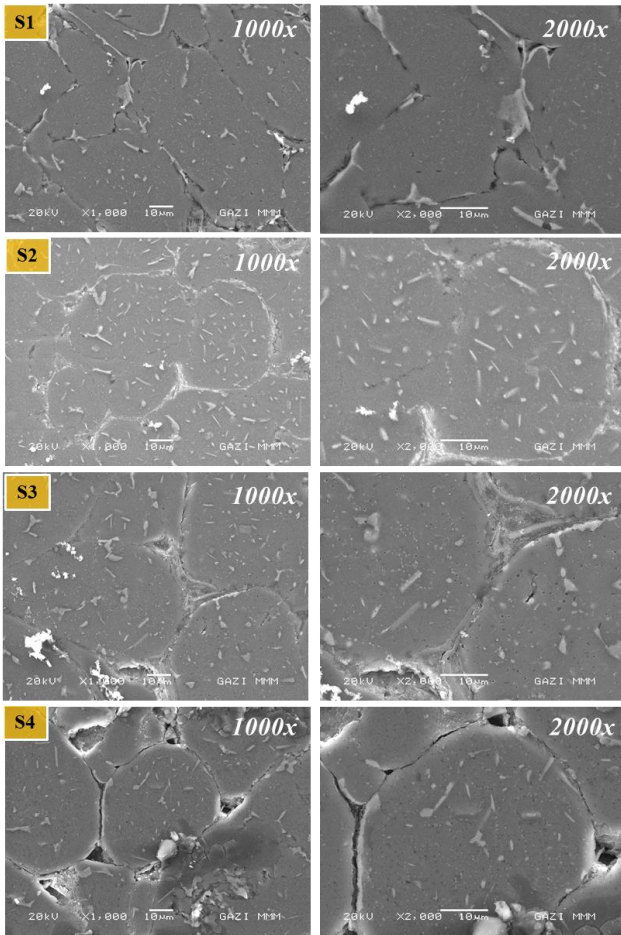


**Figure 3:** SEM images composite materials (S1: %100 AA2024, S2: %94 AA2024, %6 ZrO<sub>2</sub>, S3: %99,5 AA2024, %0,5 CNT, S4: %93,5 AA2024, %6 ZrO<sub>2</sub>, %0,5 CNT).

In the image of sample S3 with 0.5% CNT reinforcement, thin, fibre-like structures were observed. These structures are typical linear structures formed by carbon nanotubes (CNT) in SEM images. Due to the low CNT ratio, achieving a homogeneous distribution within the matrix can be difficult. The image shows that some CNTs are clustered and there are difficulties in homogeneous distribution. Local weaknesses or crack initiation points may occur where CNT is not uniformly distributed in the matrix. Therefore, the homogeneous distribution of reinforcement particles is extremely important. The hybrid structure of sample S4 (93.5% AA2024 + 6% ZrO<sub>2</sub> + 0.5% CNT) exhibited a structure in which both ZrO<sub>2</sub> and CNT reinforcements are present together. The image shows the presence of shiny ZrO<sub>2</sub> particles and fibre-like CNT structures in the same matrix. However, using these two reinforcements together also made homogeneous distribution difficult. The clustering tendency of ZrO<sub>2</sub> and localized densification of CNT are evident in the SEM images of the S4 sample belonging to the hybrid structure. The tendency of these reinforcements to accumulate, especially at the grain boundaries, may lead to microstructural problems such as bond weaknesses and crack formation. The regions where micro cracks or pores are concentrated indicate that the reinforcement materials are not fully bonded during the process. For this reason,

controlled production, such as mixing processes and hot pressing, which allow for more homogeneous reinforcement distributions, can produce more positive results in producing these materials. When all microstructure images are evaluated in general, it is observed that there is a homogeneous structure in sample S1, but in samples S2, S3 and especially S4, the homogeneous distribution of the reinforcements is not fully achieved, and agglomerations are formed in places. Since uniform dispersion of reinforcements such as ZrO<sub>2</sub> and CNT is critical for the mechanical and microstructural performance of composite materials, these difficulties in dispersion have shown that the production parameters (mixing time, ultrasonic dispersion, etc.) should be revised and re-optimized. In this context, mixing methods such as ultrasonic or longer-duration mechanical mixing can be optimized to ensure homogeneous dispersion of the reinforcements, and more controlled production atmospheres such as hot isostatic pressing can be created.

The graphs obtained from the XRD analysis applied to the composite materials are given in Figure 4.

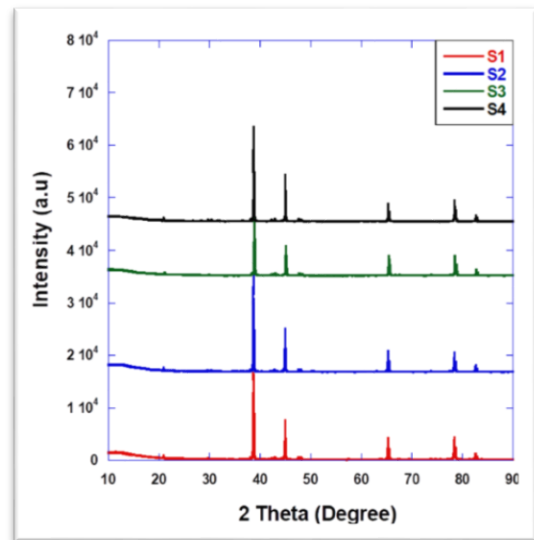


**Figure 4:** XRD graphs of composite materials

In the XRD analysis, typical peaks belonging to the AA2024 matrix were determined, and the Al peaks were observed at  $2\theta$  angles of 20.90°, 38.69°, 44.91°, 65.26°, 78.40° and 82.60°, respectively. The primary matrix material S1, indicated by red lines, clearly showed peaks specific to the AA2024 alloy in the graph. The intense peaks in the structure reflect the aluminium matrix's dominance and the crystal structure's regularity. The peaks indicate the aluminium phase with FCC (Face-Centered Cubic) structure. Since there was no other second phase or reinforcement material, S1 was evaluated as the base structure and shed light on the examinations of other samples. In the S2 (94% AA2024 + 6% ZrO<sub>2</sub>) sample drawn in blue in the graph, new peaks indicating the presence of ZrO<sub>2</sub> in addition to the AA2024 matrix were observed. ZrO<sub>2</sub> generally crystallizes in tetragonal and/or monoclinic structures. The graph reflected these structures as the displacement of the peaks or the formation of new peaks. The

appearance of distinct peaks belonging to  $ZrO_2$  showed that the reinforcement material was present in the matrix well enough to be detected in XRD analysis. The peak intensities appear consistent with the amount of  $ZrO_2$  distributed in the matrix. In the S3 sample (99.5% AA2024 + 0.5% CNT) shown with the green line in the graph, the main phase peaks of AA2024 are preserved. CNT (carbon nanotubes) generally exhibit amorphous structure properties. Therefore, it is not expected that CNT will form a clear peak in the graph. However, in some cases, weak and broad peaks specific to the graphitic structures of CNT (usually around  $2\text{-}\theta = \sim 26^\circ$ ) can be observed. In this graph, this region can be seen as a slight increase in intensity. It is also understood from the graph that CNT does not make a significant contribution to the overall XRD pattern due to its low ratio (0.5%). In the S4 sample shown with a black line in the graph (93.5% AA2024 + 6%  $ZrO_2$  + 0.5% CNT), it was observed that the peaks belonging to the AA2024 matrix were preserved, and the peaks of  $ZrO_2$  were clearly present as in S2. This situation shows that  $ZrO_2$  was still present in detectable amounts in the matrix. The presence of CNT did not seem to provide a clear contribution to the XRD pattern due to its low ratio (0.5%) and amorphous structure. This is an expected result. The S4 sample exhibited a structure combining the features of S2 and S3. However, the peak intensities showed that the effect of  $ZrO_2$  was more dominant. In XRD analyses, there are firm peaks belonging to the AA2024 matrix in all samples (S1-S4), which confirms that the matrix is dominant as the main structure in each sample. Peaks belonging to  $ZrO_2$  were clearly seen in S2 and S4 samples. These peaks show that  $ZrO_2$  exists as a crystalline phase in the matrix. Although CNT does not create clear peaks in the XRD graph due to its amorphous structure, it caused small intensity changes in S3 and S4 when the raw data were examined. When Excel data were examined, weak peaks specific to the graphitic structure were observed. In the S4 sample, the contribution of  $ZrO_2$  was evident, while CNT had little effect due to its amorphous character. The prominence of the crystalline phase peaks of  $ZrO_2$  seen in the S2 and S4 samples indicates a homogeneous distribution. However, the agglomeration regions seen in SEM images disrupt this homogeneity in places. Since the effect of CNT on the XRD pattern is limited, CNT analysis can be done with different methods (e.g. Raman spectroscopy). In XRD graphics, the compatibility of  $ZrO_2$  with the matrix was observed well as a crystalline phase. It is known from previous studies that the contribution of CNT to the phase is low but can make a difference in microstructural and mechanical properties.

#### 4. Conclusions

In this study, hybrid composite materials with AA2024 matrix and CNT -  $ZrO_2$  reinforcement were produced using powder metallurgy techniques. The materials' microstructural properties were investigated in detail with OM - SEM images and XRD graphs. The results obtained from the study are reported as follows.

1- When all microstructure images are evaluated in general, it is observed that there is a homogeneous structure

in sample S1, but in samples S2, S3 and especially S4, the homogeneous distribution of the reinforcements is not fully achieved, and agglomerations are formed in places.

2- In the OM images, S1 shows a homogeneously distributed matrix structure. The fact that there are visibly few pores and/or secondary phases in the structure indicates that the sintering process and the interface form are as expected. The grains are clearly distinguishable in the unreinforced AA2024 alloy, and the phase boundaries are well-defined.

3- In the OM images of the S2 specimen, it is observed that  $ZrO_2$  particles are dispersed in the AA2024 matrix and form dark areas. The OM images of the S3 sample determined that CNT was not wholly dispersed and formed some local densities in places. The OM images of the S4 sample show that  $ZrO_2$  and CNT reinforcements were distributed in black areas within the matrix structure. Agglomeration of  $ZrO_2$  and localized densification of CNT are observed in the images.

4- Sample S1 exhibited a homogeneous structure as in SEM images. The grain boundaries are clearly visible in the images, and no second phase or reinforcement particles were observed. In the SEM images of sample S2, many shiny, rod-like or diffusely dispersed white phases were observed. In the image of sample S3, thin, fibre-like structures were observed. The hybrid structure of sample S4 exhibited a structure in which both  $ZrO_2$  and CNT reinforcements are present. The images show the presence of shiny  $ZrO_2$  particles and fibre-like CNT structures in the same matrix.

5- In XRD analyses, there are firm peaks belonging to the AA2024 matrix in all samples (S1-S4), which confirms that the matrix is dominant as the main structure in each sample. Peaks belonging to  $ZrO_2$  were clearly seen in S2 and S4 samples. These peaks show that  $ZrO_2$  exists as a crystalline phase in the matrix. Although CNT does not create clear peaks in the XRD graph due to its amorphous structure, it caused small intensity changes in S3 and S4 when the raw data were examined.

#### References

- [1] Çalığılı U, Çanakçı A, Türkmen M, Darcan N, Kaçmış MV (2023) Investigation of the microstructure and mechanical properties of AA2024 matrix composites reinforced with  $Al_2O_3$  and SiC. *International Journal of Industrial Engineering Applications* 7(1):101–112. <https://doi.org/10.46460/ijiea.1227533>
- [2] Safa H, Güler H, Aksoy M, Şeker S (2020) Production and characterization of Al/CNT nanocomposites via powder metallurgy method. *Fırat University Journal of Science* 32(2):31–36.
- [3] Şenel MC, Üstün M (2022) Comparison of tribological properties of Al-SiO<sub>2</sub> and Al-ZrO<sub>2</sub> nanocomposites under dry sliding conditions. *OMU Journal of Engineering Sciences and Technology* 2(2):171–184.
- [4] Şenel MC, Üstün M (2022) Comparison of mechanical properties and microstructures of

- SiO<sub>2</sub>/ZrO<sub>2</sub> nanoparticle-reinforced aluminum matrix composites. *Yüzüncü Yıl University Journal of the Institute of Science* 27(2):219–232.
- [5] Şenel MC, Şenbaş T (2024) Investigation of microstructure and mechanical properties of CNT-reinforced Al6061 matrix composites produced by powder metallurgy and hot pressing. *Black Sea Journal of Science* 14(2):669–682. <https://doi.org/10.31466/kfbd.1420694>
- [6] Şahin Y (2006) Introduction to composite materials. Ankara: Seçkin Publications.
- [7] Chawla KK (2006) Composite materials. New York: Springer.
- [8] Erdoğan M (2005) Production of steel-reinforced aluminum composites and experimental investigation of their mechanical properties (Master's thesis). Dumlupınar University, Graduate School of Natural Sciences, Kütahya.
- [9] Çalin R, Muharrem P, Çitak R, Şeker U (2011) Effect of reinforcement ratio on composite structure and mechanical properties in Al-MgO composites produced by melt stirring method. *Advanced Composites Letters* 20(4). <https://doi.org/10.1177/096369351102000401>
- [10] Karslıoğlu R (2019) Effect of MWCNT ratio on microstructure and mechanical properties of Al<sub>2</sub>O<sub>3</sub> matrix nanocomposites reinforced with MWCNT. *Düzce University Journal of Science and Technology* 7(3):1922–1930.
- [11] Gültekin GG, Çanakçı A, Canpolat Ö (2023) Effect of milling time and process control agent on microstructure and mechanical properties of AA2024-2 wt.% Cu metal-metal composites produced by mechanical alloying. *Metallography Microstructure and Analysis* 12:444–454. <https://doi.org/10.1007/s13632-023-00962-2>
- [12] Yan C, Xiong D, Li J (2018) Synthesis of Ni–Al–Ta composite coatings on Al alloy plates and transfer of Al powder via mechanical milling technique. *Powder Technology* 340:234–242. <https://doi.org/10.1016/j.powtec.2018.09.024>
- [13] Fang L, Zhang X, Ren L, Hu H, Nie X, Tjong J (2018) Effect of Ni addition on tensile properties of squeeze cast Al alloy A380. *Advanced Materials and Processing Technology* 4:200–209. <https://doi.org/10.1080/2374068X.2017.1411746>
- [14] Gopalakrishna HD, Narasimha Murthy HN, Krishna M, Vinod VS, Sures AV (2010) Cold expansion of holes and resulting fatigue life enhancement and residual stresses in Al 2024 T3 alloy: An experimental study. *Engineering Failure Analysis* 17:361–368. <https://doi.org/10.1016/j.engfailanal.2009.08.002>
- [15] Wei P, Chen Z, Yao S, Huang X, Li B, Chen Y, Huang Z, Lu B (2024) Enhancing strength and ductility of graphene and ZrO<sub>2</sub> nanoparticles hybrid reinforced AA2024 composite fabricated by laser powder bed fusion. *Composites Part A: Applied Science and Manufacturing* 185:108378. <https://doi.org/10.1016/j.compositesa.2024.108378>
- [16] Özbeyaz K, Kaya H, Kentli A, Şahbaz M, Ögüt S (2019) Mechanical properties and electrical conductivity performance of ECAP processed AA2024 alloy. *Indian Journal of Chemical Technology* 26:266–269.
- [17] Kök M (2006) Abrasive wear of Al<sub>2</sub>O<sub>3</sub> particle-reinforced 2024 aluminum alloy composites fabricated by vortex method. *Composites Part A: Applied Science and Manufacturing* 37:457–464. <https://doi.org/10.1016/j.compositesa.2005.05.038>
- [18] Carreño-Gallardo C, Estrada-Guel I, López-Meléndez C, Martínez-Sánchez R (2014) Dispersion of silicon carbide nanoparticles in a AA2024 aluminum alloy by a high-energy ball mill. *Journal of Alloys and Compounds* 586:68–72. <https://doi.org/10.1016/j.jallcom.2013.03.232>
- [19] Shin JH, Choi HJ, Bae DH (2014) The structure and properties of 2024 aluminum composites reinforced with TiO<sub>2</sub> nanoparticles. *Materials Science and Engineering A* 607:605–610. <https://doi.org/10.1016/j.msea.2014.04.038>
- [20] Carreño-Gallardo C, Estrada-Guel I, Romero-Romo M, Cruz-García R, López-Meléndez C, Martínez-Sánchez R (2012) Characterization of Al<sub>2</sub>O<sub>3</sub>NP-Al 2024 and Ag CNP-Al 2024 composites prepared by mechanical processing in a high-energy ball mill. *Journal of Alloys and Compounds* 536:26–30. <https://doi.org/10.1016/j.jallcom.2011.12.010>
- [21] Zheng R, Hao X, Yuan Y, Wang Z, Ameyama K, Ma C (2013) Effect of high volume fraction of B<sub>4</sub>C particles on the microstructure and mechanical properties of aluminum alloy-based composites. *Journal of Alloys and Compounds* 576:291–298. <https://doi.org/10.1016/j.jallcom.2013.04.141>
- [22] Sameezadeh M, Emamy M, Farhangi H (2011) Effects of particulate reinforcement and heat treatment on the hardness and wear properties of AA2024-MoSi<sub>2</sub> nanocomposites. *Materials & Design* 32(4):2157–2164. <https://doi.org/10.1016/j.matdes.2010.11.037>
- [23] Bekheet NE, Galderab RM, Salah MF, Abd El-Azim AN (2002) The effects of aging on the hardness and fatigue behavior of 2024 Al alloy/SiC composites. *Materials & Design* 23(2):153–159. [https://doi.org/10.1016/S0261-3069\(01\)00072-3](https://doi.org/10.1016/S0261-3069(01)00072-3)
- [24] Yazdipour A, Heidarzadeh A (2016) Effect of friction stir welding on microstructure and mechanical properties of dissimilar Al 5083–H321 and 316L stainless steel alloy joints. *Journal of Alloys and Compounds* 680:595–603. <https://doi.org/10.1016/j.jallcom.2016.03.307>
- [25] Shayan M, Eghbali B, Niroumand B (2019) Synthesis of AA2024-(SiO<sub>2</sub>np+TiO<sub>2</sub>np) hybrid nanocomposite via stir casting process. *Materials Science and Engineering A* 756:484–491. <https://doi.org/10.1016/j.msea.2019.04.089>
- [26] Gopi Krishna M, Praveen Kumar K, Naga Swapna M, Babu Rao J, Bhargava NRM (2017) Metal-metal composites—an innovative way for multiple strengthening. *Mater Today Proc* 4:8085–8095. <https://doi.org/10.1016/j.matpr.2017.06.467>

- [27] Zuo G, Bai Y, Shi S, Tan Z, Fan W, Li Z, Hao H (2024) Interfacial healing behavior of CNTs/Al composites in solid-state additive forging. *J Manuf Process* 125:143–154. <https://doi.org/10.1016/j.jmapro.2024.07.048>
- [28] Wan J, Chen B, Zhou X, Cao L, Geng H, Shen J, Bahador A, Kondoh K, Li J (2024) CNT-induced heterogeneous matrix grain structure in CNTs/Al composites. *Carbon* 216:118529. <https://doi.org/10.1016/j.carbon.2023.118529>
- [29] Wang X, Liu L, Wang X, Bai X, Qin J, Li X, Wang B (2024) Joule heat induced ultrafine ZrO<sub>2</sub>/C composites for enhanced microwave absorption. *Surf Interfaces* 51:104818. <https://doi.org/10.1016/j.surfin.2024.104818>
- [30] Jithin PV, Dhamodaran A, Prajisha KP, Suman S, Sankaran KJ, Ramesh A, Sudheendran K, Kurian J (2025) Structural and optical properties of Ce-stabilized tetragonal phase and intense blue emission of monoclinic phase in ZrO<sub>2</sub> nanoparticles. *J Lumin* 277:120933. <https://doi.org/10.1016/j.jlumin.2024.120933>
- [31] Varol T, Çanakçı A, Özşahin Ş, Beder M, Akçay SB (2024) Prediction of the effect of fabrication parameters on the properties of B<sub>4</sub>C ceramic particle reinforced AA2024 matrix nanocomposites using neural networks. *Mater Today Commun* 39:109279. <https://doi.org/10.1016/j.mtcomm.2024.109279>
- [32] Uyar E, Akay D, Pul M (2024) Investigation of radiation shielding properties of Al<sub>2</sub>O<sub>3</sub>, Zn<sub>2</sub>(Zamac), and Cu composites reinforced with nano graphene and multi-walled carbon nanotubes. *SSRN*. <https://doi.org/10.2139/ssrn.4805836>
- [33] Stergioudi F, Prospathopoulos A, Farazas A, Tsirogiannis EC, Michailidis N (2022) Mechanical properties of AA2024 aluminum/MWCNTs nanocomposites produced using different powder metallurgy methods. *Metals* 12(8):1315. <https://doi.org/10.3390/met12081315>
- [34] Channar HR, Ullah B, Naseem MS, Akhter J, Mehmood A, Aamir M (2024) Mechanical properties and microstructural investigation of AA2024-T6 reinforced with Al<sub>2</sub>O<sub>3</sub> and SiC metal matrix composites. *Eng* 5(4):3023–3032. <https://doi.org/10.3390/eng5040157>
- [35] Akgümüş Gök D, Bayraktar C, Hoşkun M (2024) A review on processing, mechanical, and wear properties of Al matrix composites reinforced with Al<sub>2</sub>O<sub>3</sub>, SiC, B<sub>4</sub>C, and MgO by powder metallurgy method. *J Mater Res Technol* 31:1132–1150. <https://doi.org/10.1016/j.jmrt.2024.06.110>
- [36] Sarmah P, Gupta K (2024) Recent advancements in fabrication of metal matrix composites: A systematic review. *Materials (Basel)* 17(18):4635. <https://doi.org/10.3390/ma17184635>
- [37] Özerkan HB, Subaşı M, Pul M (2024) Investigation of machinability by electrical discharge machining method of ZA27/MWCNT composites produced by powder metallurgy. *Sigma* 42(6):1965-1972. <https://doi.org/10.14744/sigma.2024.00160>
- [38] Elbasuney S, Gobara M, Zoriany M, Maraden A, Naeem I (2019) The significant role of stabilized colloidal ZrO<sub>2</sub> nanoparticles for corrosion protection of AA2024. *Environ Nanotechnol Monit Manag* 12:100242. <https://doi.org/10.1016/j.enmm.2019.100242>
- [39] Singh AP, Kumar MS, Deshpande A, Jain G, Khamesra J, Mhetre S, Awasthi A, Natrayan L (2021) Processing and characterization mechanical properties of AA2024/Al<sub>2</sub>O<sub>3</sub>/ZrO<sub>2</sub>/Gr reinforced hybrid composite using stir casting technique. *Mater Today Proc* 37(2):1562–1566. <https://doi.org/10.1016/j.matpr.2020.07.156>